Commun Nonlinear Sci Numer Simulat 29 (2015) 482–487

Contents lists available at ScienceDirect

Commun Nonlinear Sci Numer Simulat

journal homepage: www.elsevier.com/locate/cnsns

From localized spots to the formation of invaginated labyrinthine structures in a Swift–Hohenberg model

I. Bordeu[a,*], M.G. Clerc[b], R. Lefever[c], M. Tlidi[c]

[a] Departamento de Física, Facultad de Ciencias, Universidad de Chile, Santiago, Chile
[b] Departamento de Física, Facultad de Ciencias Físicas y Matemáticas, Universidad de Chile, Casilla 487-3, Santiago, Chile
[c] Département de Physique, Faculté des Sciences, Université Libre de Bruxelles (U.L.B.), CP 231, Campus Plaine, B-1050 Bruxelles, Belgium

ARTICLE INFO

Article history:
Received 6 April 2015
Revised 27 May 2015
Accepted 28 May 2015
Available online 5 June 2015

Keywords:
Nonlinear dynamics
Pattern formation in complex systems

ABSTRACT

The stability of a circular localized spot with respect to azimuthal perturbations is studied in a prototype variational model, namely, a Swift–Hohenberg type equation. The conditions under which the circular shape of the spot undergoes an elliptical deformation which transforms it into a rod-shaped structure are analyzed. As it elongates, the rod structure exhibits a transversal instability, generating an invaginated labyrinthine structure which invades all the space available.

1. Introduction

Several spatially extended systems that undergo a symmetry breaking instability close to a second-order critical point can be described by real order parameter equations in the form of Swift–Hohenberg type of models. These models, have been derived in various fields of nonlinear science such as hydrodynamics [1], chemistry [2], plant ecology [3], nonlinear optics [4–6], and elastic materials [7].

A complex Swift–Hohenberg equation was deduced in the context of lasers [8–10] and optical parametric oscillators [11]. Moreover, to describe the nascent optical bistability with transversal effect in nonlinear optical cavities a real approximation has been deduced [12] from laser equations. This approximation allowed the prediction of stable, single and clustered localized structures [12]. A detailed derivation of this equation from first principles can be found in Ref. [8]. In the present work, we show that this real modified Swift–Hohenberg equation (SHE) of the form

$$\partial_t u = \eta + \epsilon u - u^3 - \nu \nabla^2 u - \nabla^4 u \tag{1}$$

supports a curvature instability over localized structures that lead to an elliptical deformation, producing a rod-like structure. With the temporal evolution, the rod-like structure exhibits a transverse undulation, leading to the formation of invaginated structures. Such a structure is a labyrinthine pattern, characterized by its interconnected structure where the field value is high. The outer region or complement to the invaginated structure corresponds to low field value. This behavior occurs far from any pattern forming instability and requires a bistable behavior between homogeneous steady states. In Eq. (1), $u = u(x, y, t)$ is a real scalar field, x and y are spatial coordinates and t is time.

The parameter η represents the external forcing field which brakes the reflection symmetry $u \to -u$. The bifurcation parameter is ϵ. The coefficient ν may change the sign of the diffusive term ∇^2, and allows the pattern forming to take place [4,13–17].

* Corresponding author. Tel.: +56 978879738.
E-mail address: ibordeu@gmail.com (I. Bordeu).

http://dx.doi.org/10.1016/j.cnsns.2015.05.028
1007-5704/

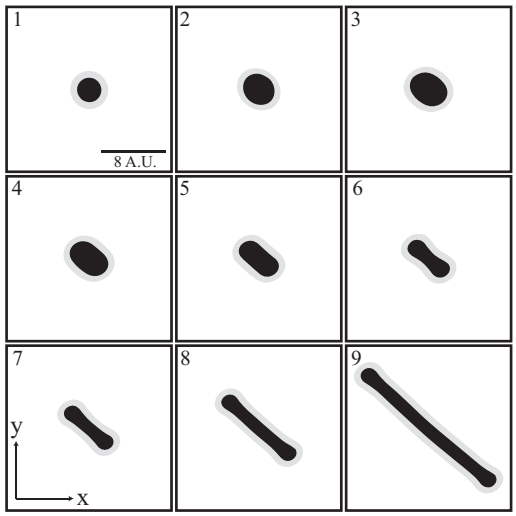

Fig. 1. Temporal evolution for; (1) $t = 0$; (2) $t = 125$; (3) $t = 175$; (4) $t = 225$; (5) $t = 275$; (6) $t = 340$; (7) $t = 350$; (8) $t = 360$; (9) $t = 400$, of a localized spot through an elliptical deformation into a rod-like structure for Eq. (1) with: $\eta = -0.065$; $\epsilon = 2.45$; $\nu = 2.0$. Minima are plain white. The image corresponds to a zoom of 16×16 points of a 512×512 points finite-difference simulation, with Neumann boundary conditions.

Depending on the context in which this equation is derived, the physical meaning of the field variable and parameters adopt particular meanings, for instance, in cavity nonlinear optics $u(x, y, t)$ corresponds to light field intensity, while parameters $\{\eta, \epsilon, \nu\}$ are associated with the injection field, the deviations of the cavity field, and cooperativity, respectively [12].

For certain ranges of parameter values, Eq. (1) exhibits stable circular localized structures. General properties such as existence, stability and dynamical evolution of these structures have been well studied (see Refs. [18–27]). Recent review on localized structures can be found in [28]. For $\eta < 0$ localized structures emerge as isolated peaks of the field $u(x, y, t)$, instead, for $\eta > 0$ localized structures appear as holes in the field. These localized structures have a fixed stable radius for each parameter value. Curvature instability of localized spot has been experimentally studied or theoretically predicted in magnetic fluids [29], liquid crystals [30,31], reaction–diffusion systems [32–40,40–43], plant ecology [44], material science [45,46], granular fluid systems and frictional fluids [47,48], and nonlinear optics [49]. The fingering instability of planar fronts leading to the formation of labyrinth structures has been reported by Hagberg et al. [50]. In this manuscript we shall focus on circular localized states.

2. Stability of localized spots

Considering fixed parameter values, starting with an azimuthally symmetric stationary localized structure. The structure is then perturbed, this perturbation grows radially as shown in Fig. 2(1). The circular shape becomes unstable at some critical radius. The elliptical shape elongate into a rod-like structures as shown in Fig. 1. This elongation proceeds until a critical size is reached beyond which a transversal instability onset the appearance of fingers near the midsection of the structure (see Fig. 2(3)). The finger continues their elongation, and the amplitude of oscillation increases (Fig. 2(4) and (5)). The dynamic of the system does not saturate and for a long time evolution, the rod-like structure invades the whole space available in (x, y)-plane as shown in Fig. 2(6). This invaginated structure is stationary solutions of the SHE. The dynamic described previously has been observed in cholesteric liquid crystals under the presence of an external electric field [30,31], where an initially circular structure of cholesteric phase suffers from a curvature instability, transversal oscillations and develops into an extended labyrinthine structure. The characterization of this dynamic is an open problem.

For $\nu = 2$, the bifurcation diagram of the model Eq. (1) in the parameter space (ϵ, η) is shown in Fig. 3. For $\epsilon > 0$ the system undergoes a bistable regime between homogeneous steady states. For $\epsilon < 0$, the system possesses only one homogeneous steady state. The curve Γ_1 represents the pitchfork bifurcation, where the coordinates of the limit points of the bistable curve are given by $\eta_\pm = \pm 2(\epsilon/3)^{3/2}$. The threshold associated with a symmetry breaking or Turing instability is provided by the curve Γ_2. The coordinates of the symmetry breaking instabilities thresholds are $\eta_\pm = \pm\sqrt{(\nu^2 + 4\epsilon)/3}(\nu^2 - 8\epsilon)/24$. The Γ_1 and Γ_2 curves are well known in the literature [51,52]. We have built numerically the curve Γ_3, which separates the zone of bistability where localized structures are stable, zone II, from the zone where they are unstable, zone I. The transition from localized structures to labyrinthine patterns take place when crossing from the I-zone to the II-zone, through the Γ_3-curves indicated in Fig. 3. This transition occurs via fingering instability at the Γ_3-curves delimiting the parameter domain I and II. In the limit of the classical Swift–Hohenberg equation, $\eta = 0$, there is no observation of fingering instability, instead, at the transition from II-zone to I-zone, localized structures only grow radially. The destabilization of these structures into labyrinthine structures may be observed, as a result of size effect phenomenon due to boundary conditions. In contrast, for $\eta \neq 0$ the transition from the II-zone to the I-zone

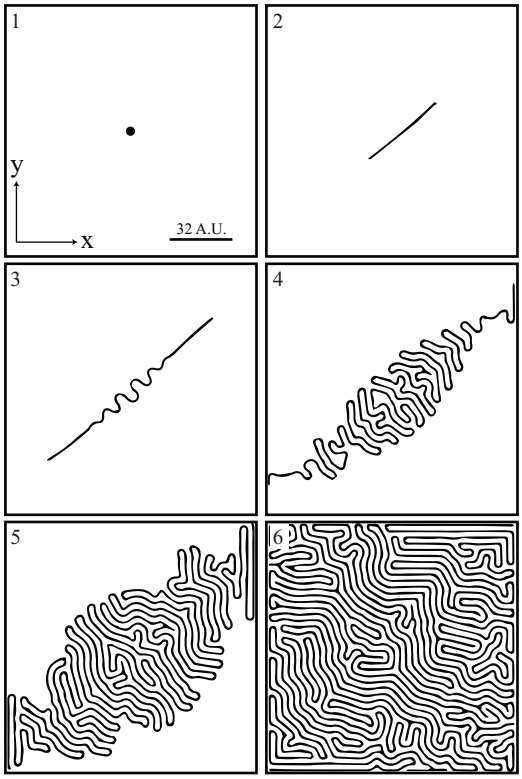

Fig. 2. Transition from a single localized spot to invaginated pattern. Temporal evolution with Neumann boundary conditions and with the same parameters as in Fig. 1. (1) $t = 0$, localized spot, (2) $t = 600$, rod-like structure, (3) $t = 1900$, transverse undulation of the rod-like structure, (4) $t = 2800$, (5) $t = 3700$, localized transient patterns, and (6) $t > 15{,}000$, stationary invaginated labyrinth pattern. Minima are plain white and the mesh integration is 512×512 points. Simulation done with finite-difference method.

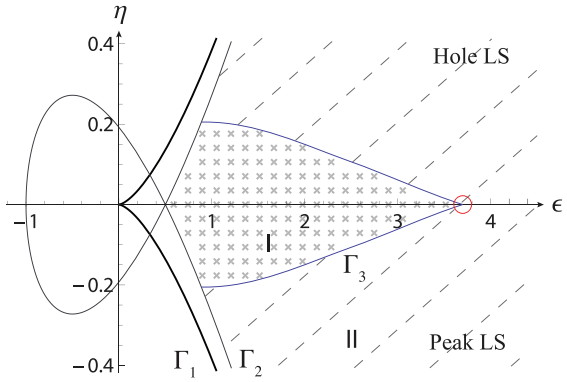

Fig. 3. Bifurcation diagram of Eq. (1) in (ϵ, η) space for $\nu = 2.0$. In II-zone (dashed black), stable circular localized structures are observed. In I-zone (gray crosses) generation of labyrinthine structures are observed from localized structures. The transition curve Γ_3 was constructed numerically.

of a localized spot induces a curvature instability, giving rise to an unstable rod structure which exhibits transversal oscillations and develops into an extended labyrinthine structure.

In what follows, we first study the stability of a circular localized spot with respect to azimuthal perturbations. This linear analysis allows us to evaluate the threshold above which the transition from localized spot to a rod-like structure takes place. Then, a linear stability analysis of the rod-like structure is performed, to determine the conditions under which the transversal oscillations occur for the SH equation.

Starting from a stationary solution with rotational symmetry (i.e. circular localized structure) $u = u_s(r)$ where r is the radial coordinate. Then, the solution is perturbed $u(r, \theta, t) = u_s(r) + \delta u(r) e^{\lambda_m t} \cos(m\theta)$, where θ is the angular coordinate, and $\delta u(r) \ll 1$. It should be noted that the perturbation mode $m = 2$ represents an elongation of the circular structure into an elliptical shape. Using polar representation of Eq. (1), considering the above perturbation and parameters in Eq. (1) at linear order in W

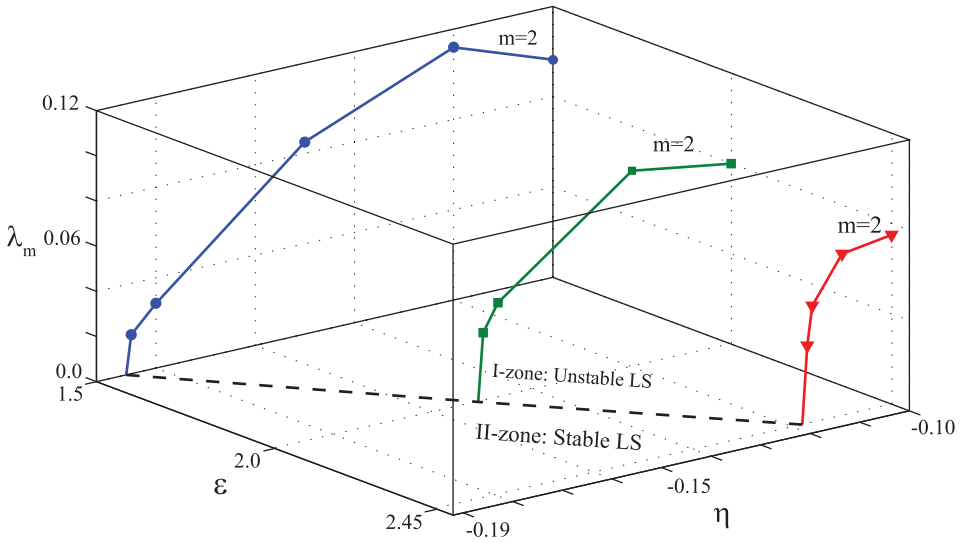

Fig. 4. Dots show the growth rate λ_m of the most unstable perturbation mode obtained numerically for different values of ϵ. Dashed line separates zones of stable and unstable localized structures (see Fig. 3). Parameters: $\nu = 2$; $dx = 0.5$; $dt = 0.03$. Periodic boundary conditions were used.

one obtains

$$\frac{\partial W}{\partial t} = \mathcal{L}W \tag{2}$$

where the linear operator $\mathcal{L} \equiv \epsilon + 3u_s^2(r) - \nu\nabla^2 - \nabla^4$ is explicitly dependent on the radial coordinate. Analytical calculations are not accessible when the operator is inhomogeneous.

However, by direct simulation of Eq. (1) with an initially stationary localized structure one can find the growth rate of the most unstable mode. First for fixed values of the parameters $\{\eta, \epsilon, \nu\}$ a stationary localized spot is considered as initial condition. Note that the radius of localized spot is determined by a balance between the interface energy and the energy difference between the homogeneous states which are proportional to ν and η, respectively. The radius of the localized structures r_s is proportional to ν/η [53]. Afterwards, the system is perturbed by homogeneous noise, this type of perturbation can be regarded as a linear combination of all the angular modes m. However, the most unstable mode (the one with largest eigenvalue λ_m) dominates the temporal dynamics and is the only one observable. By considering the stability of the localized spot for different values of the parameter η under homogeneous noise perturbations we can determine that the most unstable mode ($\lambda_2 > 0$) is $m = 2$ as observed in Fig. 4. This mode deforms the circular localized spot into an elliptically shaped structure as shown in Fig 2(2).

3. Transversal instability of rod structures and emergence of labyrinthine patterns

The SHE Eq. (1) admits a single stripe-like solution [21,54]. In order to evaluate the threshold over which transversal oscillations appear, we perform the stability analysis of a rod-like structure, by a method similar to the one performed in Ref. [50]. For this purpose we perturb the single stripe solution as $u = u_f(\boldsymbol{\xi}) + W(\boldsymbol{x}, \boldsymbol{X_0})$ where u_f is the single stripe solution and $\boldsymbol{\xi} = \boldsymbol{x} - \boldsymbol{X_0}(y, t)$ the relative position, $\boldsymbol{X_0}$ is the field that accounts for the shape and evolution of the rod, and $W(\boldsymbol{x}, \boldsymbol{X_0}) \ll 1$ is a non-linear correction of a single stripe. Applying this ansatz in Eq. (1) at first order in W and applying the solvability condition [16], the following equation is obtained for the dynamic of $\boldsymbol{X_0}$

$$\partial_t X_0 = -\Delta'\partial_{yy}X_0 + 6\beta'\partial_y^2 X_0(\partial_y X_0)^2 - \partial_y^4 X_0, \tag{3}$$

where

$$\beta' = \frac{\langle \partial_{\xi\xi} u_f | \partial_{\xi\xi} u_f \rangle}{\langle \partial_\xi u_f | \partial_\xi u_f \rangle}, \text{ and } \Delta' = (\nu - 2\beta'). \tag{4}$$

Thus $\boldsymbol{X_0}$ satisfies a nonlinear diffusion equation. This equation describes the dynamics of an interface between two symmetric states [55,56]. This model is well known for exhibiting a zigzag instability. Analogously, to the previous section, when $\Delta < 0$ the single stripe solution is stable, and for $\Delta > 0$, the solution is unstable as result of the curvature instability. From Eq. (3) one expects to observe the single stripe becomes unstable by the emergence of undulations. Fig. 5 illustrates the manifestation of this undulations under the consideration of an infinitely long rod-like structure, to avoid border effects. Note that similar dynamical behavior is observed in the propagation of cholesteric finger in liquid crystals [30,31]. Later, this undulated stripe is replaced by the emergence of facets that form a zigzag structure. However the higher nonlinear terms control the evolution of the single stripe, then the dynamics of initial zigzag is replaced by the growth of undulations without saturation as it is depicted in Fig. 2(4).

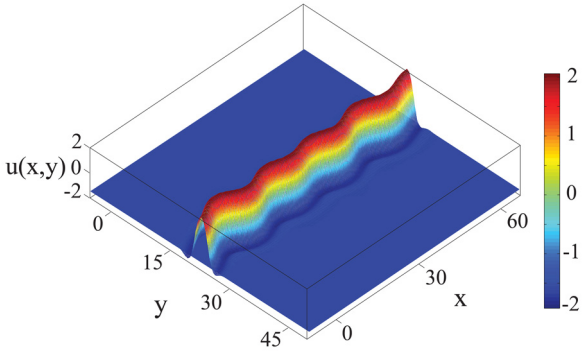

Fig. 5. Transversal instability of a single infinite stripe of Eq. (1). Image shows a section of a 256 × 256 points simulation with boundary conditions using a pseudo-spectral code. Parameters: $\eta = -0.065$, $\epsilon = 2.45$, $\nu = 2$, $dx = 0.5$, and $dt = 0.03$.

Therefore, the system displays the emergence of a roll-like transverse pattern which is formed in the midsection of the structure and invades the system generating invaginated structure (see Fig. 2(5)).

4. Conclusions

In this paper we have described the stability of localized spot in a modified Swift–Hohenberg equation. First, the bifurcation diagram was constructed, showing the possible solutions that appear in different parameter regimes. Afterwards, it was shown that the angular index $m = 2$ becomes unstable as consequence of curvature instability. Such instability leads to an elliptical deformation of the localized spot.

When angular index $m = 2$ becomes unstable, the curvature instability of localized spot produces an elliptical deformation leading to the generation of a rod-like structure. Subsequently, it causes undulations in the rod-like structure. The spatiotemporal evolution leads to the formation of invaginated labyrinthine structures. To understand this dynamics, we have performed the analytical stability analysis of a single stripe localized structure.

It should be noted that by an offset transformation, $u \to u + u_0$, where u_0 is a constant, Eq. (1) can be rewritten in such a way that the constant parameter η is removed and a quadratic nonlinearity appears. This quadratic model is equivalent to Eq. (1). The model with a quadratic nonlinearity has been well studied (see the textbook [16] and the references therein). This equivalence implies that the results of the present work are also valid for physical systems described by the quadratic model.

Acknowledgments

M.G.C. thanks the financial support of FONDECYT project 1150507. I.B. thanks the support from CONICYT, Beca de Magister Nacional and the Departamento de Postgrado y Postítulo of the Vicerrectoria de Asuntos Académicos, Universidad de Chile. M.T. received support from the Fonds National de la Recherche Scientifique (Belgium). M.T acknowledges the financial support of the Interuniversity Attraction Poles program of the Belgian Science Policy Office, under grant IAP 7–35 photonics@be.

References

[1] Swift J, Hohenberg PC. Phys Rev A 1977;15:319.
[2] Hilali M'F, Dewel G, Borckmans P. Phys Lett A 1996;217:263.
[3] Lefever R, Barbier N, Couteron P, Lejeune O. J Theor Biol 2009;261:194.
[4] Tlidi M, Georgiou M, Mandel P. Phys Rev A 1993;48:4605.
[5] Kozyreff G, Chapman SJ, Tlidi M. Phys Rev E 2003;68:015201.
[6] Clerc MG, Petrossian A, Residori S. Phys Rev E 2005;71:015205(R).
[7] Stoop N, Lagrange R, Terwagne D, Reis PM, Dunkel J. Nat Mater 2015;14:337.
[8] Mandel P. Theoretical problems in cavity nonlinear optics. New York: Cambridge University Press; 1997.
[9] Lega J, Moloney JV, Newell AC. Phys Rev Lett 1994;73:2978.
[10] Lega J, Moloney JV, Newell AC. Physica D 1995;83:478.
[11] Longhi S, Geraci A. Phys Rev A 1996;54:4581.
[12] Tlidi M, Mandel P, Lefever R. Phys Rev Lett 1994;73:640.
[13] Cross MC, Hohenberg PC. Rev Mod Phys 1993;65:851.
[14] Hohenberg PC, Halperin BI. Rev Mod Phys 1977;49:435.
[15] Aranson IS, Malomed BA, Pismen LM, Tsimring LS. Phys Rev E 2000;62:R5.
[16] Pismen LM. Patterns and interfaces in dissipative dynamics. Berlin, Heidelberg: Springer Series in Synergetics; 2006.
[17] Vladimirov AG, Lefever R, Tlidi M. Phys Rev A 2011;84:043848.
[18] Aranson IS, Gorshkov KA, Lomov AS, Rabinovich MI. Physica D 1990;43:435.
[19] Glebsky LYu, Lerman LM. Chaos 1995;5:424.
[20] Hilali MF, Métens S, Borckmans P, Dewel G. Phys Rev E 1995;51:2046.
[21] Tlidi M, Mandel P, Lefever R. Phys Rev Lett 1998;81:979.
[22] Coullet P, Riera C, Tresser C. Phys Rev Lett 2000;84:3069.
[23] Richter R, Barashenkov IV. Phys Rev Lett 2005;94:184503.

[24] Burke J, Knobloch E. Phys Rev E 2006;73:056211.
[25] Lloyd DJB, Sandstede B, Avitabile D, Champneys AR. J Appl Dyn Syst 2008;7:1049.
[26] McCalla S, Sandstede B. Physica D 2010;239:1581.
[27] Knobloch E. Annu Rev Condens Matter Phys 2015;6:325.
[28] Tlidi M, Staliunas K, Panajotov K, Vladimiorv AG, Clerc M. Phil Trans R Soc A 2014;372:20140101.
[29] Dickstein AJ, Erramilli S, Goldstein RE, Jackson DP, Langer SA. Science 1993;261:1012.
[30] Ribiere P, Oswald P. J Phys 1990;51:1703.
[31] Oswald P, Baudry J, Pirkl S. Phys Rep 2000;337:67.
[32] Pearson JE. Science 1993;261:189.
[33] Lee K, McCormick WD, Pearson JE, Swinney HL. Nature (London) 1994;369:215.
[34] Munuzuri AP, Perez-Villar V, Markus M. Phys Rev Lett 1997;79:1941.
[35] Kaminaga A, Vanag VK, Epstein IR. Angew Chem 2006;45:3087.
[36] Kaminaga A, Vanag VK, Epstein IR. J Chem Phys 2005;122:174706.
[37] Kolokolnikov T, Tlidi M. Phys Rev Lett 2007;98:188303.
[38] Davis PW, Blanchedeau P, Dulos E, De Kepper P. J Phys Chem A 1998;102:8236.
[39] Muratov CB, Osipov VV. Phys Rev E 1996;53:3101; Muratov CB. Phys Rev E 2002;66:066108.
[40] Monine M, Pismen L, Bar M, Or-Guil M. J Chem Phys 2002;117:4473.
[41] Schaak A, Imbihl R. Chem Phys Lett 1998;283:368.
[42] Hayase Y, Ohta T. Phys Rev Lett 1998;81:1726.
[43] Hayase Y, Ohta T. Phys Rev E 2000;62:5998.
[44] Meron E, Gilad E, von Hardenberg J, Shachak M. Chaos Solitons Fractals 2004;19:367.
[45] Ren X, Wei J. SIAM J Math Anal 2003;35:1.
[46] Nishiura Y, Suzuki H. SIAM J Math Anal 2004;36:916.
[47] Sandnes B, Knudsen HA, Maloy KJ, Flekkoy EG. Phys Rev Lett 2007;99:038001.
[48] Sandnes B, Flekkoy EG, Knudsen HA, Maloy KJ, See H. Nat Commun 2011;2:288.
[49] Tlidi M, Vladimirov AG, Mandel P. Phys Rev Lett 2002;89:233901.
[50] Hagberg A, Yochelis A, Yizhaq H, Elphick C, Pismen L, Meron E. Physica D 2006;217:186.
[51] Coullet P, Riera C, Tresser C. Prog Theor Phys Suppl 2000;139:46.
[52] del Campo F, Haudin F, Rojas RG, Bortolozzo U, Clerc MG, Residori S. Phys Rev E 2012;86:036201.
[53] Coullet P. Int J Bifur Chaos 2002;12:2445.
[54] Tlidi M, Mandel P, Le Berre M, Ressayre E, Tallet A, Di Menza L. Opt Lett 2000;25:487.
[55] Chevallard C, Clerc M, Coullet P, Gilli J-M. Europhys Lett 2002;58:686.
[56] Calisto H, Clerc M, Rojas R, Tirapegui E. Phys Rev Lett 2000;85:3805.